

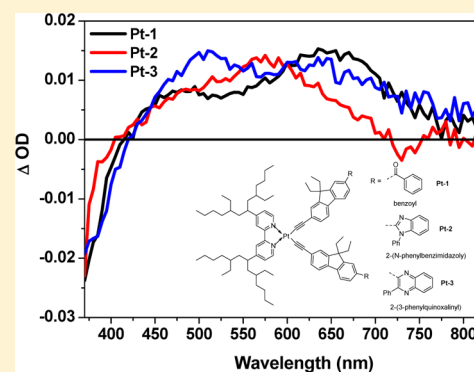
# Synthesis, Photophysics, and Reverse Saturable Absorption of Bipyridyl Platinum(II) Bis(acetylide) Complexes Bearing Aromatic Electron-Withdrawing Substituents on the Acetylide Ligands

Xu-Guang Liu and Wenfang Sun\*

Department of Chemistry and Biochemistry, North Dakota State University, Fargo, North Dakota 58108-6050, United States

## Supporting Information

**ABSTRACT:** Three platinum(II) bipyridyl bis((7-*R*-fluorenyl)acetylide) complexes (*R* = benzoyl (Pt-1), 2-(*N*-phenylbenzimidazolyl) (Pt-2), or 2-(3-phenylquinoxaliny) (Pt-3)) are synthesized and characterized. Their photophysical properties and reverse saturable absorption are systematically investigated via UV-vis absorption, emission, transient absorption, and nonlinear transmission spectroscopy/technique. All three complexes possess ligand-centered  $^1\pi,\pi^*$  transitions below 400 nm, and a broad, featureless  $^1\text{MLCT}/^1\text{LLCT}$  absorption band in the region of 400–550 nm in  $\text{CH}_2\text{Cl}_2$  solutions. They are emissive in a variety of fluid solutions at room temperature and at 77 K glassy matrix. On the basis of the emission lifetime, solvatochromic effect, and thermally induced Stokes shift, the emitting states are tentatively ascribed to  $^3\pi,\pi^*/^3\text{MLCT}/^3\text{LLCT}$  states for Pt-1, and predominantly  $^3\text{MLCT}/^3\text{LLCT}$  states for Pt-2 and Pt-3 in polar solvents like  $\text{CH}_3\text{CN}$ . Pt-1–Pt-3 also exhibit broad triplet excited-state absorption, i.e., 425–800 nm for Pt-1 and Pt-3, and 425–725 nm for Pt-2, from the same excited states that emit. Strong reverse saturable absorption (RSA) occurs at 532 nm for ns laser pulses from all of the complexes due to the stronger triplet excited-state absorption at this wavelength, suggesting that the  $\pi$ -conjugated aromatic electron-withdrawing substituents at the fluorenylacetylide ligands enhance the RSA of the Pt(II) diimine bis(acetylide) complexes.



## INTRODUCTION

Platinum diimine bis(acetylide) complexes<sup>1</sup> possess unique photophysical properties, like phosphorescence in fluid solutions at room temperature and broadband excited-state absorption. These photophysical properties along with the square-planar configuration around the Pt(II) center make these complexes promising candidates for applications in photocatalysis,<sup>2</sup> photoinduced charge separation,<sup>3</sup> vapoluminescence,<sup>4</sup> OLEDs,<sup>5</sup> upconversion,<sup>6,7</sup> nonlinear optics,<sup>8–16</sup> etc. It is well understood that the photophysics of the Pt(II) diimine acetylide complexes, like the ground-state absorption, the emission energy and lifetime, and the triplet excited-state absorption and lifetime, depends on the structure of the acetylide ligands<sup>1,8–20</sup> that can be readily modified. Therefore, it is possible to tune the ground-state and excited-state properties of the platinum diimine acetylide complexes to meet the requirement of a specific application by variation of the acetylide ligands.

A variety of aromatic substituents attached to the acetylide ligands, including phenyl,<sup>1,10,17–20</sup> naphthyl,<sup>21</sup> anthryl,<sup>17</sup> pyrenyl,<sup>22</sup> perylenyl,<sup>17</sup> fluorenyl,<sup>6–9,11–16</sup> naphthalimide,<sup>23,24</sup> coumarinyl,<sup>25</sup> and naphthaldiimide,<sup>26</sup> have been studied. The different aryl substituents not only affect the ground-state absorption of the Pt(II) diimine acetylide complexes significantly but also alter the nature of the lowest triplet

excited state dramatically. The influence of different auxiliary substituents on the phenylacetylide ligands have been investigated by Eisenberg<sup>18,20</sup> and Schanze<sup>19</sup> groups independently. It was found that strong electron-withdrawing substituent like  $\text{NO}_2$  or strong electron-donating substituent like  $\text{NMe}_2$  alters both the singlet and triplet excited-state properties drastically. Very recently, our group reported the tuning of photophysical properties of Pt(II) diimine bis(stilbenylacetylide) complexes<sup>10</sup> and Pt(II) diimine bis(fluorenylacetylide) complexes by auxiliary substituents.<sup>11</sup> It was also revealed that strong electron donor or acceptor on the acetylide ligands could influence the excited-state energy and lifetimes dramatically.

The reported work on the Pt(II) diimine bis(acetylide) complexes is very exciting. However, limited work has reported the nonlinear absorption of these complexes. In 2010, our group first reported the reverse saturable absorption (RSA) and two-photon absorption (TPA) of a Pt(II) bipyridyl complex bearing bis(benzothiazolylfluorenylacetylide) ligands.<sup>8,9</sup> We found that this complex exhibited strong RSA in the visible

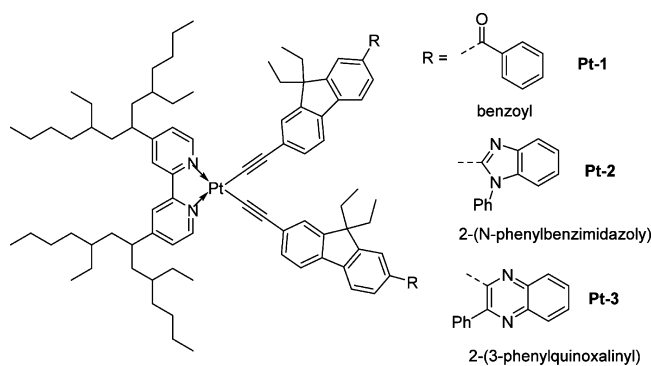
**Special Issue:** Current Topics in Photochemistry

**Received:** January 13, 2014

**Revised:** March 10, 2014

spectral region and two-photon initiated excited-state absorption in the near-IR region.<sup>8</sup> Later, we discovered that Pt(II) bipyridyl complexes with electron-withdrawing substituents, such as NO<sub>2</sub> and naphthalimide, attached at the fluorenyl-acetylide ligands possessed much broader excited-state absorption;<sup>11,16</sup> and extended  $\pi$ -conjugation in the acetylide ligands could increase the triplet excited-state lifetime and consequently enhance the excited-state absorption in the visible spectral region.<sup>13–15</sup> Inspired by these results, we intend to further improve the nonlinear absorption of the Pt(II) bipyridyl complexes by fine-tuning the  $\pi$ -conjugated aromatic electron-withdrawing auxiliary substituent at the fluorenyl-acetylide ligands (structures of the complexes are shown in Chart 1).

**Chart 1. Chemical Structures of Pt(II) Bipyridyl Complexes Pt-1–Pt-3**



Benzoyl, 2-(*N*-phenylbenzimidazolyl), and 2-(3-phenylquinoxaliny) are chosen for this study because fluorene derivatives with these substituents were demonstrated to exhibit moderate TPA.<sup>28</sup>

## EXPERIMENTAL SECTION

**Materials and Synthesis.** The reagents and solvents for synthesis were obtained from Alfa Aesar or Aldrich Chemical Co. and used as received unless otherwise noted. Nuclear magnetic resonance (NMR) spectroscopy was used to characterize the intermediates, while <sup>1</sup>H NMR, <sup>13</sup>C NMR, HRMS, and elemental analyses were used to characterize the platinum complexes Pt-1–Pt-3.

A Varian Oxford-400 VNMR or a Varian Oxford-500 VNMR spectrometer was used to measure the NMR spectra for all of the intermediates and the Pt complexes; and a Bruker Autoflex Speed MALDI-TOF mass spectrometer was used to obtain the HRMS data for Pt-1–Pt-3. Elemental analyses were conducted

by NuMega Resonance Laboratories, Inc., in San Diego, California.

**Ligand Synthesis.** Schemes 1–3 depict the synthetic routes for the acetylide ligands L-1–L-3. The details of the synthetic procedure and characterization data are reported in the Supporting Information.

The precursor **1** in Scheme 1 was prepared in two steps from fluorene according to the reported procedures.<sup>28</sup> Then **1** was first ethylated to obtain compound **2** in 75% yield. Subsequent reaction of **2** with benzonitrile followed by hydrolysis of the product under acidic conditions gave the benzoyl substituted intermediate **3**, which is a mixture of bromo- and iodo-substituted product. The Sonogashira coupling reaction of **3** with ethynyltrimethylsilane followed by hydrolysis with K<sub>2</sub>CO<sub>3</sub> afforded the ligand L-1.

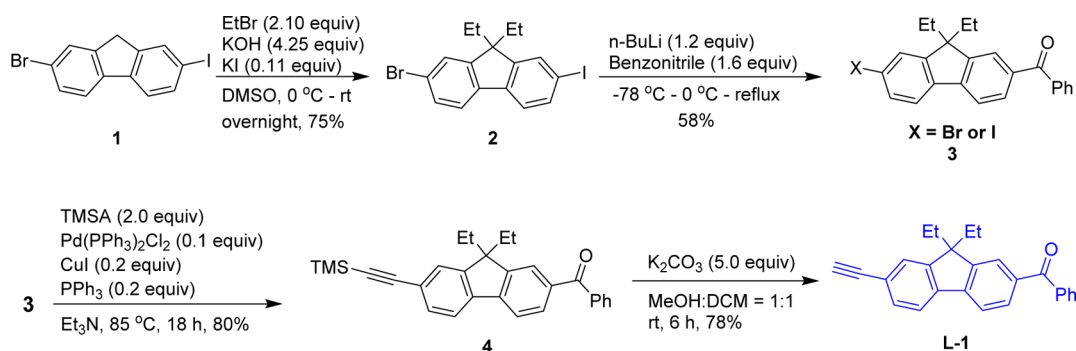
As depicted in Scheme 2, ligand L-2 was synthesized from 9,9-diethyl-2,7-diiodo-9*H*-fluorene (**6**), which was prepared from fluorene in two steps.<sup>29</sup> Then, the halogen–metal exchange reaction of compound **6** with *n*-butyllithium followed by reaction with DMF produced the aldehyde (**7**) in 43% yield. Reaction of compound **7** with *N*-phenyl-1,2-phenylenediamine (**9**), which was prepared from *o*-fluoronitrobenzene in two steps, followed by oxidation with copper(II) acetate, produced the *N*-phenylbenzimidazole intermediate **10**.<sup>30</sup> Finally Sonogashira coupling reaction of **10** with ethynyltrimethylsilane followed by hydrolysis with K<sub>2</sub>CO<sub>3</sub> afforded the ligand L-2.

The syntheses of L-3 utilized the same intermediate **6** as that for L-2 (see Scheme 3). Sonogashira coupling reaction between **6** and phenylacetylene afforded compound **12**, which was a mixture of mono- and disubstituted product. The mixed compound **12** was directly treated with PdCl<sub>2</sub> to obtain the diketone compound **13**, which was able to be separated from the disubstituted byproduct. Subsequently, the condensation reaction of diketone and benzene-1,2-diamine produced the 3-phenylquinoxaliny substituted intermediate **14**.<sup>31</sup> Finally, Sonogashira coupling reaction of **14** with ethynyltrimethylsilane followed by hydrolysis with K<sub>2</sub>CO<sub>3</sub> afforded ligand L-3.

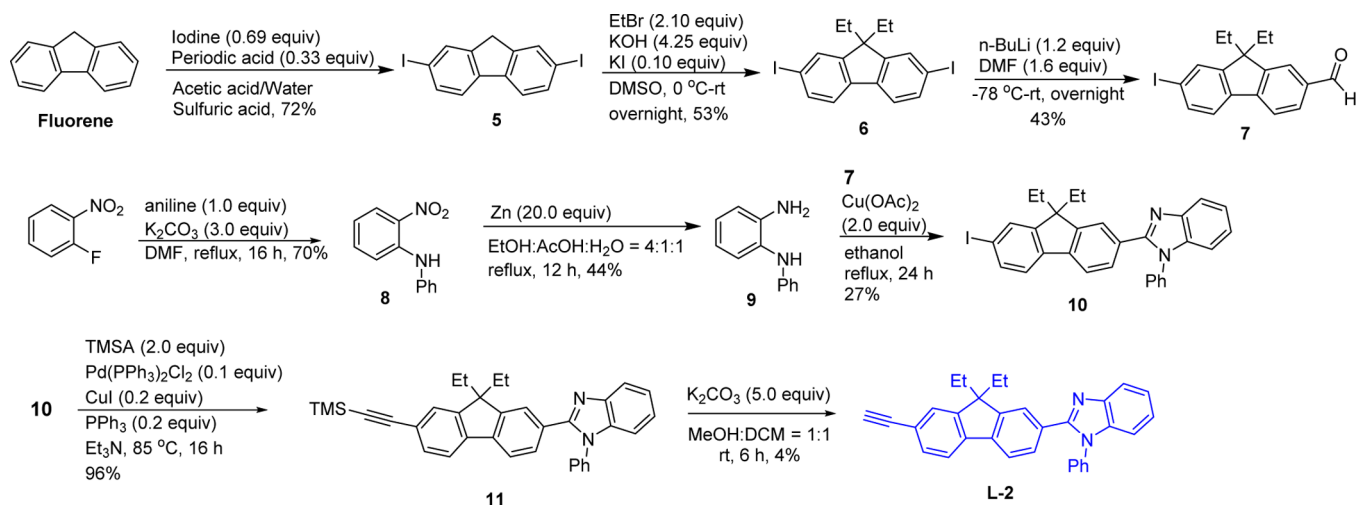
**Pt(II) Complex Synthesis.** The precursor (bpy)PtCl<sub>2</sub> was synthesized following the literature procedure.<sup>10</sup> Complexes Pt-1, Pt-2, and Pt-3 were then obtained by reaction of (bpy)PtCl<sub>2</sub> with the corresponding acetylene ligand L-1, L-2, or L-3 in the presence of diisopropylamine and CuI (Scheme 4). The products exhibit good solubility in common organic solvents due to the presence of branched alkyl chains at the bipyridine ligand, which reduce the intermolecular  $\pi$ – $\pi$  stacking.

All complexes were synthesized following this procedure: A mixture of (bpy)PtCl<sub>2</sub> (1.0 equiv), ligand L-*x* (*x* = 1, 2, or 3) (2.0 equiv), and CuI (0.10 equiv) in mixed dichloromethane

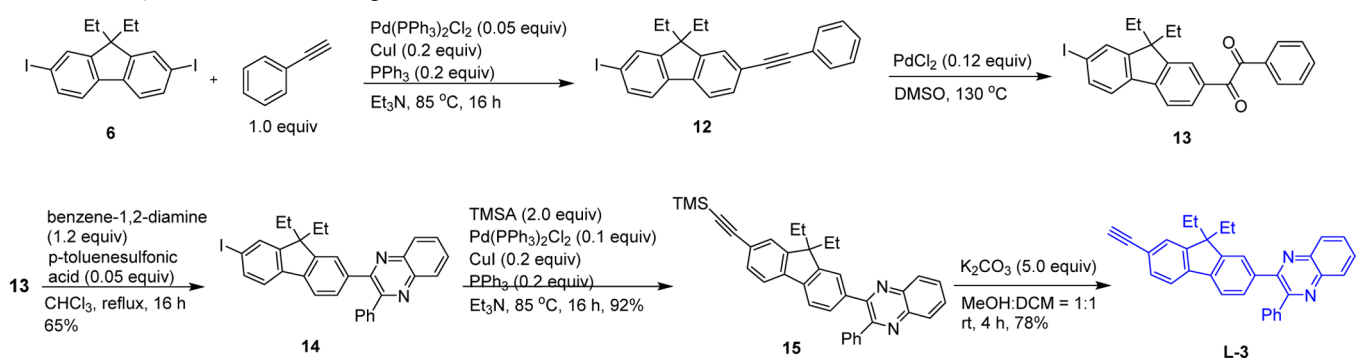
**Scheme 1. Synthetic Route for Ligand L-1**



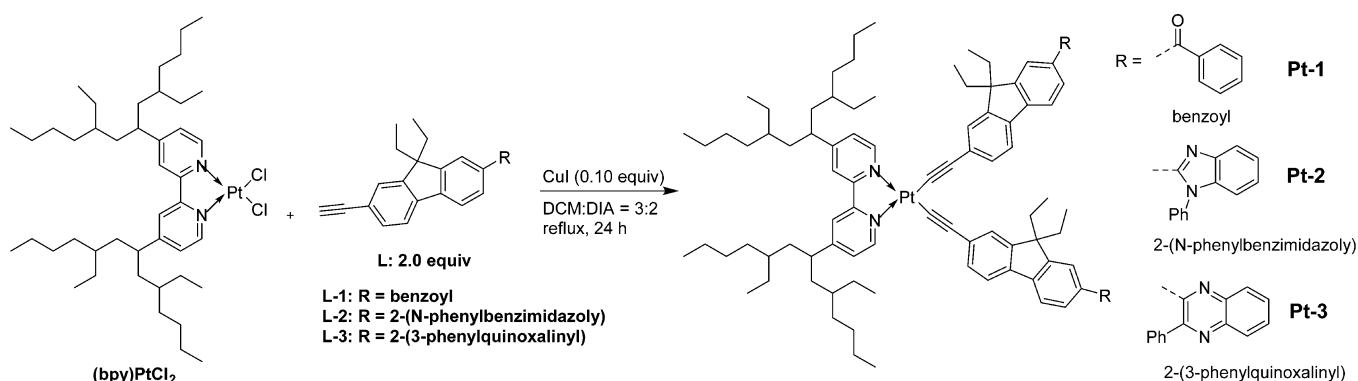
## Scheme 2. Synthetic Route for Ligand L-2



## Scheme 3. Synthetic Route for Ligand L-3.



## Scheme 4. Synthetic Route for Pt(II) Complexes Pt-1–Pt-3



and diisopropylamine (v/v = 3:2) was refluxed under argon atmosphere for 24 h. After that, the reaction mixture was cooled to room temperature. The solvent was removed and the residue was extracted with dichloromethane. The CH<sub>2</sub>Cl<sub>2</sub> layer was washed with water and dried over anhydrous Na<sub>2</sub>SO<sub>4</sub>. Then the solvent was removed and the residue was purified by column chromatography (silica gel; the eluent used was hexane/ethyl acetate = 1:0–4:1–3:1 (v/v)).

**Pt-1.** Starting from 147 mg of (bpy)PtCl<sub>2</sub>, 140 mg of orange solid was obtained as the product (yield: 56%). <sup>1</sup>H NMR (500 MHz, CDCl<sub>3</sub>): δ 0.38 (t, J = 7.0 Hz, 12H, CH<sub>3</sub>), 0.81–0.93 (m, 24H, CH<sub>3</sub>), 1.09–1.41 (m, 34H, CH<sub>2</sub>), 1.58–1.62 (m, 8H, CH<sub>3</sub>), 2.07 (q, J = 7.0 Hz, 8H, CH<sub>2</sub>), 2.94–2.96 (m, 2H, CH),

7.46 (d, J = 5.5 Hz, 2H, Ar), 7.51 (t, J = 7.5 Hz, 4H, Ar), 7.58–7.62 (m, 6H, Ar), 7.69 (d, J = 7.5 Hz, 2H, Ar), 7.73 (d, J = 8.0 Hz, 2H, Ar), 7.78–7.80 (m, 4H, Ar), 7.82–7.84 (m, 6H, Ar), 9.81 (d, J = 5.5 Hz, 2H, Ar). <sup>13</sup>C NMR (100 MHz, CDCl<sub>3</sub>): δ 8.4, 10.1, 10.7, 14.0, 22.9, 23.0, 25.1, 26.1, 28.2, 28.7, 32.2, 32.5, 32.9, 36.0, 36.3, 40.5, 40.6, 41.2, 41.3, 56.2, 87.6, 103.2, 118.8, 119.9, 120.9, 126.8, 127.0, 128.1, 128.4, 129.9, 130.1, 131.4, 131.9, 135.3, 137.6, 138.5, 146.3, 150.1, 150.6, 151.4, 156.2, 160.0, 196.8. HRMS: *m/z* Calcd for [C<sub>96</sub>H<sub>118</sub>N<sub>2</sub>O<sub>2</sub>Pt]<sup>+</sup>, 1525.8894; found, 1525.8700. Anal. Calcd for C<sub>96</sub>H<sub>118</sub>N<sub>2</sub>O<sub>2</sub>Pt: C, 75.51; H, 7.79; N, 1.83. Found: C, 75.13; H, 7.72; N, 1.93%.

**Pt-2.** Starting from 19 mg of (bpy)PtCl<sub>2</sub>, 20 mg of orange solid was obtained as the product (yield: 54%). <sup>1</sup>H NMR (500 MHz, CDCl<sub>3</sub>): δ 0.18 (t, *J* = 7.5 Hz, 12H, CH<sub>3</sub>), 0.77–0.93 (m, 24H, CH<sub>3</sub>), 1.08–1.43 (m, 34H, CH<sub>2</sub>), 1.56–1.78 (m, 16H, CH<sub>3</sub>), 1.86–1.94 (m, 4H, CH<sub>2</sub>), 2.91–2.94 (m, 2H, CH), 7.26–7.29 (m, 6H, Ar), 7.33–7.36 (m, 6H, Ar), 7.42–7.54 (m, 12H, Ar), 7.58 (d, *J* = 7.5 Hz, 2H, Ar), 7.63 (d, *J* = 8.0 Hz, 2H, Ar), 7.7–7.72 (m, 4H, Ar), 7.91 (d, *J* = 8.0 Hz, 2H, Ar). <sup>13</sup>C NMR (100 MHz, CDCl<sub>3</sub>): δ 8.4, 10.1, 10.7, 14.0, 14.1, 22.9, 23.1, 25.1, 26.2, 28.2, 28.7, 32.2, 32.6, 32.9, 36.1, 36.3, 40.6, 41.3, 56.0, 86.8, 103.3, 110.3, 119.3, 119.7, 120.9, 122.9, 123.1, 123.9, 126.9, 127.5, 127.6, 128.3, 128.6, 129.8, 131.2, 137.2, 137.4, 138.1, 143.08, 143.12, 149.7, 149.8, 151.4, 153.3, 156.2, 159.9. HRMS: *m/z* Calcd for [C<sub>108</sub>H<sub>126</sub>N<sub>6</sub>Pt]<sup>+</sup>, 1701.9744; found, 1701.9795. Anal. Calcd for C<sub>108</sub>H<sub>126</sub>N<sub>6</sub>Pt·0.5CH<sub>2</sub>Cl<sub>2</sub>·(iPr)<sub>2</sub>NH: C, 74.46; H, 7.75; N, 5.31. Found: C, 74.12; H, 6.91; N, 5.77%.

**Pt-3.** Starting from 68 mg of (bpy)PtCl<sub>2</sub>, 30 mg of orange solid was obtained as the product (yield: 23%). <sup>1</sup>H NMR (500 MHz, CDCl<sub>3</sub>): δ 0.18 (t, *J* = 7.0 Hz, 12H, CH<sub>3</sub>), 0.78–0.92 (m, 24H, CH<sub>3</sub>), 1.07–1.40 (m, 34H, CH<sub>2</sub>), 1.60–1.69 (m, 16H, CH<sub>3</sub>), 1.83–1.89 (m, 4H, CH<sub>2</sub>), 2.91–2.94 (m, 2H, CH), 7.13 (s, 2H, Ar), 7.32–7.33 (m, 6H, Ar), 7.42 (d, *J* = 5.5 Hz, 2H, Ar), 7.51 (s, 2H, Ar), 7.54–7.57 (m, 6H, Ar), 7.63 (d, *J* = 7.5 Hz, 2H, Ar), 7.72–7.79 (m, 8H, Ar), 7.82 (d, *J* = 8.0 Hz, 2H, Ar), 8.17–8.22 (m, 4H, Ar), 9.79 (d, *J* = 5.0 Hz, 2H, Ar). <sup>13</sup>C NMR (100 MHz, CDCl<sub>3</sub>): δ 8.5, 10.1, 10.7, 14.0, 14.1, 22.9, 23.1, 25.1, 26.2, 28.2, 28.7, 32.2, 32.5, 32.9, 36.0, 36.3, 40.5, 40.6, 40.7, 41.2, 41.3, 56.0, 86.6, 103.3, 119.3, 119.7, 120.9, 127.8, 126.8, 126.9, 127.4, 128.4, 128.6, 128.7, 129.1, 129.6, 129.8, 131.1, 136.9, 138.3, 139.5, 141.0, 141.3, 142.6, 149.5, 149.8, 151.4, 153.8, 154.0, 156.2, 159.8, 159.9. HRMS: *m/z* Calcd for [C<sub>110</sub>H<sub>126</sub>N<sub>6</sub>Pt]<sup>+</sup>, 1725.9744; found: 1725.9788. Anal. Calcd for C<sub>110</sub>H<sub>126</sub>N<sub>6</sub>Pt: C, 76.49; H, 7.35; N, 4.87. Found: C, 76.45; H, 6.99; N, 5.07%.

**Photophysical Measurements.** The UV–vis absorption spectra and steady-state emission spectra of Pt-1–Pt-3 were measured in different HPLC grade solvents. An Agilent 8453 spectrophotometer was used for the UV–vis absorption measurement, and a SPEX fluorolog-3 fluorometer/phosphorometer was utilized for the steady-state emission study. A comparative method<sup>32</sup> with a degassed aqueous solution of [Ru(bpy)<sub>3</sub>]Cl<sub>2</sub> (Φ<sub>em</sub> = 0.042, λ<sub>ex</sub> = 436 nm)<sup>33</sup> being used as the reference was applied to determine the emission quantum yields of Pt-1–Pt-3 in degassed solutions. An Edinburgh LP920 laser flash photolysis spectrometer was utilized to acquire the triplet excited-state lifetimes and the triplet transient difference absorption spectra in degassed solutions. The excitation source was the third harmonic output (355 nm) of a Nd:YAG laser (Quantel Brilliant, pulsewidth ≈ 4.1 ns, repetition rate was set at 1 Hz). Each sample was degassed with argon for at least 30 min prior to measurement.

**Nonlinear Transmission Measurements.** The experimental setup resembled that reported by our group before.<sup>34</sup> The second harmonic output (λ = 532 nm) of a Q-switched Quantel Brilliant Nd:YAG laser (4.1 ns (fwhm), 10 Hz) was used as the light source. The focal length of the plano-convex lens used was 30 cm, which focused the laser beam to ~96 μm (radius) at the center of a 2 mm thick sample cuvette. The incident and output energies were monitored using two Moletron J4-09 pyroelectric probes and an EPM2000 energy/power meter.

## RESULTS AND DISCUSSION

**Electronic Absorption.** The electronic absorption of L-1–L-3 and Pt-1–Pt-3 was studied in CH<sub>2</sub>Cl<sub>2</sub> at different concentrations (1 × 10<sup>-6</sup>–5 × 10<sup>-4</sup> mol/L). The Beer's law is obeyed in this concentration range by all of these compounds, indicating that neither dimerization nor oligomerization occurs at the ground state for these compounds (see Supporting Information Figure S1). Figure 1 depicts the UV–

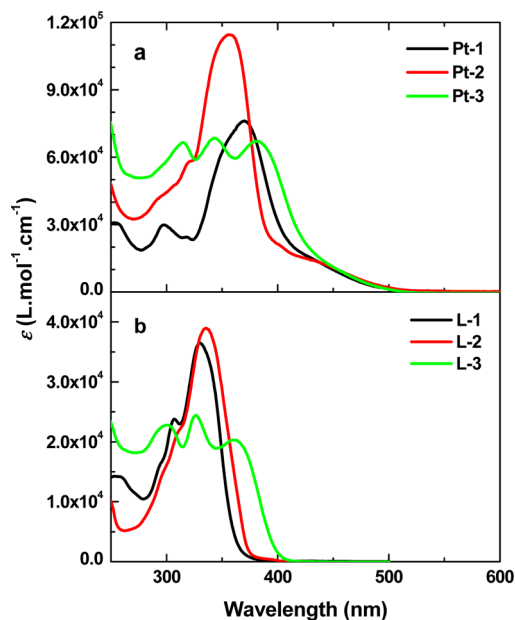


**Figure 1.** UV–vis absorption spectra of Pt-1–Pt-3 (a) and L-1–L-3 (b) in CH<sub>2</sub>Cl<sub>2</sub>.

vis absorption spectra of L-1–L-3 and Pt-1–Pt-3 in CH<sub>2</sub>Cl<sub>2</sub>, and Table 1 lists their absorption band maxima and molar extinction coefficients. In line with the Pt(II) diimine bis(acetylide) complexes reported in the literature,<sup>3–27</sup> the UV–vis absorption spectra of Pt-1–Pt-3 (Figure 1a) are composed of two groups of bands: the major absorption bands below 400 nm are ascribed to the <sup>1</sup>π,π\* transitions localized on the acetylide ligand; while the tails above 400 nm are attributed to the <sup>1</sup>LLCT (ligand-to-ligand charge transfer)/<sup>1</sup>MLCT (metal-to-ligand charge transfer) transitions. The assignment of <sup>1</sup>π,π\* transitions to the major absorption bands is supported by the facts that the energies of these bands resemble those of their corresponding acetylide ligands (Figure 1b) and that the solvatochromic effect of these bands (Figure 2 for Pt-2 and Supporting Information Figure S2 for Pt-1 and Pt-3) are quite minor. However, these bands are clearly red-shifted in comparison to those of their respective ligands, suggesting the delocalization of the ligand-centered molecular orbitals via the interactions with the platinum dπ orbitals. In contrast to the major absorption bands, the low-energy tails in these complexes shift to longer wavelengths in hexane and toluene compared to those in CH<sub>3</sub>CN and CH<sub>2</sub>Cl<sub>2</sub> (exemplified in Figure 2 for complex Pt-2), manifesting a clear negative solvatochromic effect. The negative solvatochromic effect is a characteristic feature for <sup>1</sup>LLCT/<sup>1</sup>MLCT transitions as reported for many other Pt(II) diimine bisacetylide complexes.<sup>8–16</sup>

**Emission.** Pt-1–Pt-3 are luminescent in fluid solutions at room temperature and in glassy matrix at 77 K. Figure 3 shows the normalized emission spectra of these complexes in CH<sub>2</sub>Cl<sub>2</sub>



Table 1. Photophysical Data for Pt-1–Pt-3

	$\lambda_{\text{abs}}$ (nm) <sup>a</sup> ( $\epsilon$ ( $10^4$ L·mol <sup>-1</sup> ·cm <sup>-1</sup> ))	$\lambda_{\text{em}}$ (nm) <sup>b</sup> ( $\tau$ ( $\mu$ s)); $\Phi_{\text{em}}$ rt	$\lambda_{\text{em}}$ (nm) <sup>c</sup> ( $\tau_{\text{em}}$ ( $\mu$ s)) 77 K	$\lambda_{\text{T1-Tn}}$ (nm) <sup>d</sup> ( $\tau_{\text{TA}}$ ( $\mu$ s))
Pt-1	370 (7.59), 422 (1.75)	554 (3.23); 0.33	538 (62.8), 574 (68.3)	495 (4.44), 635 (3.84)
Pt-2	356 (11.44), 415 (1.68)	570 (0.70); 0.16	528 (47.3), 565 (47.9)	575 (0.49)
Pt-3	314 (6.64), 343 (6.84), 381 (6.69), 440 (1.46)	572 (2.06); 0.15	541 (57.5), 581 (58.1)	510 (2.71), 635 (2.05)

<sup>a</sup>In CH<sub>2</sub>Cl<sub>2</sub> solution. <sup>b</sup>In CH<sub>2</sub>Cl<sub>2</sub> solution; the excitation wavelength was 436 nm. <sup>c</sup>Measured at a concentration of  $1 \times 10^{-5}$  mol/L in BuCN glassy matrix. <sup>d</sup>Measured in CH<sub>3</sub>CN.

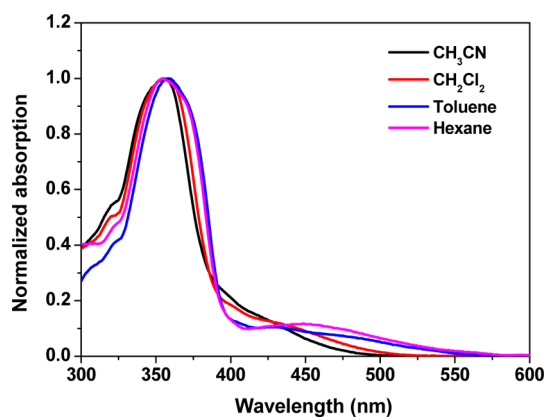


Figure 2. Normalized UV-vis absorption spectra of Pt-2 in different solvents.

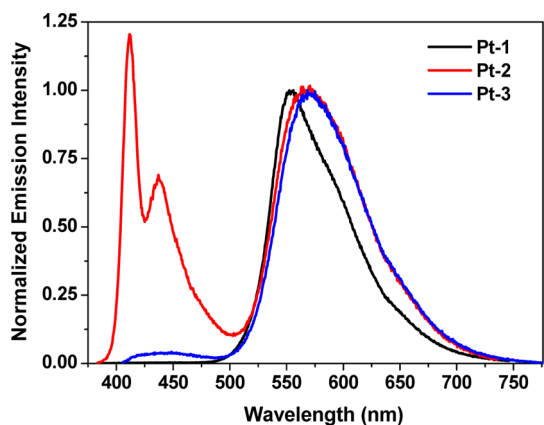


Figure 3. Normalized emission spectra of complexes Pt-1, Pt-2, and Pt-3 in CH<sub>2</sub>Cl<sub>2</sub>.  $\lambda_{\text{ex}}$  = 378 nm for Pt-1, 397 nm for Pt-2, and 396 nm for Pt-3.

at a concentration of  $1 \times 10^{-5}$  mol/L, and Table 1 lists the emission lifetimes and quantum yields. When excited at their respective charge transfer bands, all complexes exhibit a broad, structureless emission band between 500 and 750 nm with lifetimes varying from 700 ns to approximately 3  $\mu$ s in degassed CH<sub>2</sub>Cl<sub>2</sub> solutions. The Stokes shifts of these emission bands are in the range of 7650–8400 cm<sup>-1</sup> with respect to their corresponding excitation wavelengths, and this emission can be quenched by oxygen readily. Therefore, this orange–red emission is assigned to phosphorescence from a triplet excited state. Considering the shape of the emission spectrum and the emission lifetime and referring to the reported Pt(II) diimine complexes,<sup>3–27</sup> this emission can be tentatively regarded as emanating from the <sup>3</sup>MLCT/<sup>3</sup>LLCT states in CH<sub>2</sub>Cl<sub>2</sub>. However, upon excitation at their corresponding <sup>1</sup> $\pi$ , $\pi^*$  bands, complexes Pt-2 and Pt-3 exhibit dual emission, with a short-lived structured emission band at ca. 425 nm for Pt-2 and a structureless emission band at ca. 440 nm for Pt-3, except for

their phosphorescence bands. Considering the short lifetime and the similar energy of this band to their respective acetylide ligands (Supporting Information Figure S3), we assign the high-energy emission to fluorescence from the coordinated acetylide ligands.

To understand how the complex concentration affects the emission characteristics, the emission of all three complexes in dichloromethane at different concentrations was investigated. As exemplified in Figure 4 for Pt-1, the shape of the emission

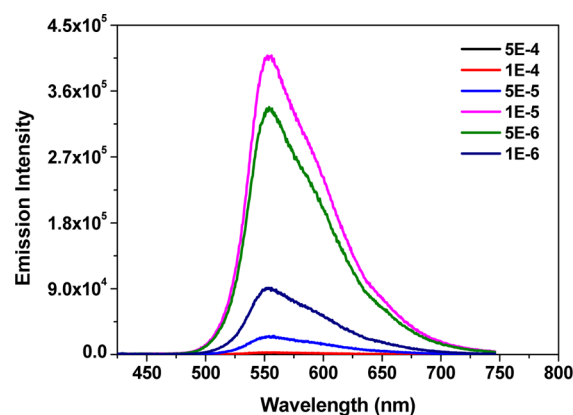


Figure 4. Concentration-dependent emission spectra of Pt-1 in CH<sub>2</sub>Cl<sub>2</sub>.  $\lambda_{\text{ex}}$  = 378 nm for Pt-1.

spectrum remains the same at different concentrations, while the intensity of the emission keeps increasing until the concentration reaches  $1 \times 10^{-5}$  mol/L. Above  $1 \times 10^{-5}$  mol/L, the emission intensity decreases. However, the emission lifetime does not change when the solution concentration varies. This indicates the absence of self-quenching at high concentrations. Because no ground-state aggregation (as demonstrated by the UV-vis absorption study) and self-quenching occur at high concentrations, the decreased emission intensity at high concentrations could be ascribed to the primary inner-filter effect,<sup>35</sup> namely, the attenuation of the excitation light by the increased absorption of molecules at the front surface of the cuvette when the sample concentration increases. Similar phenomena have been observed for Pt-2 and Pt-3 as demonstrated in Supporting Information Figure S4.

The emission characteristics of Pt-1–Pt-3 in different solvents have been studied as well. The solvent-dependent emission spectra of complex Pt-1 are presented in Figure 5, and the emission energies, lifetimes, and quantum yields in different solvents are summarized in Supporting Information Table S1. The shape of the emission spectra of Pt-1 in polar solvents such as CH<sub>3</sub>CN is different from that in less polar solvent like toluene. Clear vibronic progression with a vibronic spacing of 1007 cm<sup>-1</sup> is observed from the emission spectrum in CH<sub>3</sub>CN, and the lifetime in CH<sub>3</sub>CN is much longer than that in toluene and comparable to that in CH<sub>2</sub>Cl<sub>2</sub>. These features imply that the emitting state of Pt-1 in CH<sub>3</sub>CN is probably different from

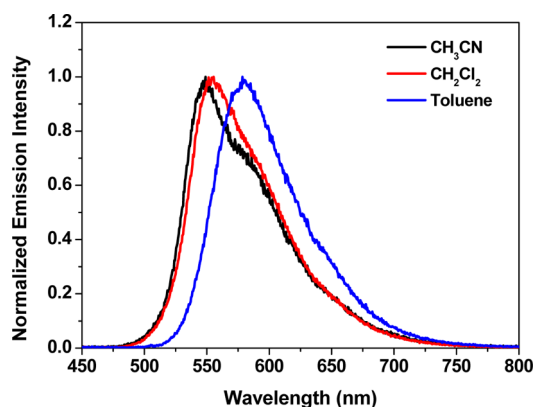


Figure 5. Solvent-dependent emission spectra of Pt-1.  $\lambda_{\text{ex}} = 436$  nm.

that in less polar solvents. The emission of Pt-1 in CH<sub>3</sub>CN likely arises from the mixed <sup>3</sup>MLCT/<sup>3</sup>LLCT/<sup>3</sup> $\pi,\pi^*$  states, while the emission in CH<sub>2</sub>Cl<sub>2</sub> and toluene seems to be dominated by the <sup>3</sup>MLCT/<sup>3</sup>LLCT states. The switching/mixing of the emitting state between <sup>3</sup>MLCT/<sup>3</sup>LLCT and <sup>3</sup> $\pi,\pi^*$  by solvent has been demonstrated by Castellano's group for the Pt(II) bipyridyl complex with naphthylacetylde ligands<sup>21</sup> and by our group for the Pt(II) bipyridyl complex with benzothiazolyl-fluorenylacetylde ligands.<sup>8</sup> Differing from Pt-1, the emission spectra of Pt-2 and Pt-3 remain featureless in both polar and nonpolar solvents (see Supporting Information Figure S5 for Pt-2 and Pt-3), and both of them manifest a negative solvatochromic effect. In addition, quenching of the emission by coordinating solvent like CH<sub>3</sub>CN is observed (as demonstrated by the decreased emission lifetime and quantum yield). Considering these two features, we believe that the emitting states of Pt-2 and Pt-3 are predominantly <sup>3</sup>MLCT/<sup>3</sup>LLCT states in both the polar and nonpolar solvents.

Complexes Pt-1, Pt-2, and Pt-3 also emit at 77 K in butyronitrile glassy matrix (shown in Figure 6 for complex Pt-1

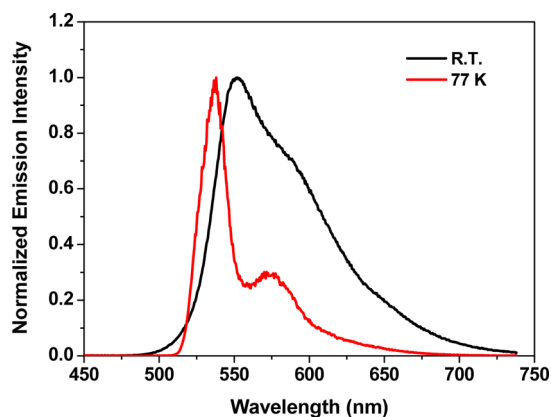


Figure 6. Comparison of emission spectra of Pt-1 at 77 K (in butyronitrile matrix) and at room temperature (in butyronitrile solution) at the concentration of  $1 \times 10^{-5}$  mol/L.  $\lambda_{\text{ex}} = 374$  nm.

and in Supporting Information Figure S6 for Pt-2 and Pt-3). The emission spectra at 77 K are narrower, clearly structured, and hypsochromically shifted with respect to their emission spectra at room temperature. The thermally induced Stokes shift is 538 cm<sup>-1</sup> for Pt-1, 1542 cm<sup>-1</sup> for Pt-2, and 1029 cm<sup>-1</sup> for Pt-3. The small thermally induced Stokes shift of Pt-1 in BuCN is consistent with the admixture of <sup>3</sup> $\pi,\pi^*$  configuration

in the emitting state in polar solvents as discussed in the previous paragraph; while the larger thermally induced Stokes shifts in Pt-2 and Pt-3 are in line with the charge transfer nature of the emitting states assigned to Pt-2 and Pt-3 earlier.

**Transient Absorption.** To gain further insight into the triplet excited state of Pt-1–Pt-3, the excited-state absorption of these complexes was investigated via nanosecond transient absorption (TA) spectroscopy. The TA spectroscopy measures the absorption difference between the ground and the excited states and thus allows one to determine the wavelength region in which the excited-state absorption is stronger than that of the ground state (which corresponds to the positive absorption bands in the TA spectrum), which is important for one to predict the spectral region where reverse saturable absorption (i.e., the absorptivity of the materials increases with increased incident energy to decrease the transmission of light) can occur. Additionally, from the decay of the TA one can obtain the lifetime of the triplet excited state giving rise to the observed TA. The nanosecond transient difference absorption spectra of complexes Pt-1–Pt-3 in degassed CH<sub>3</sub>CN solutions at zero time delay after 355 nm excitation are presented in Figure 7 and the time-resolved TA spectra of these complexes are provided in Supporting Information Figure S7.

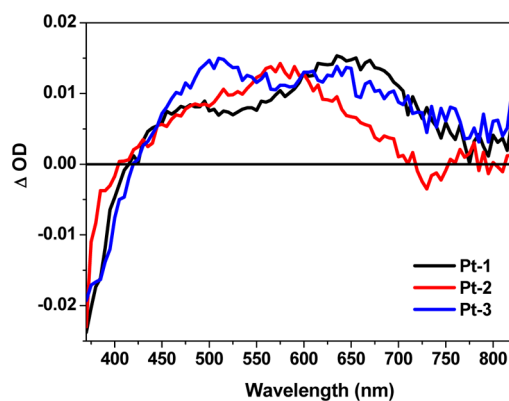
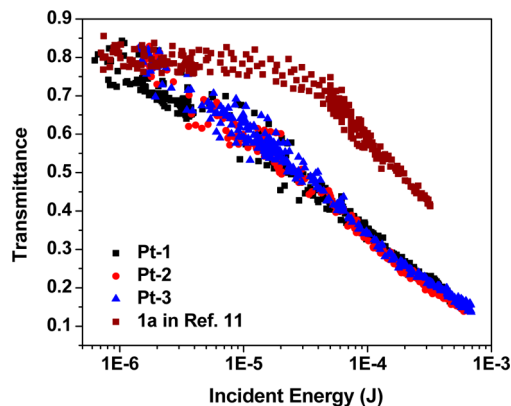


Figure 7. Nanosecond transient different absorption spectra of Pt-1–Pt-3 in degassed CH<sub>3</sub>CN solution at zero time delay following 355 nm excitation. For all measurements,  $A_{355 \text{ nm}} = 0.4$  in a 1 cm cuvette.

Figure 7 shows that Pt-1–Pt-3 possess broad positive absorption band(s) between 425 and 725 nm (the TA bands of Pt-1 and Pt-3 extend to 800 nm) and bleaching occurs below 425 nm. However, the TA shape of Pt-2 differs from those of Pt-1 and Pt-3. Pt-2 only possesses one broad absorption band centered at 575 nm, while the spectra of Pt-1 and Pt-3 contain two TA bands, one at ca. 500 nm and another one at ca. 630 nm. Considering the similar lifetimes obtained from the decay of the TA to those from the decay of emission in the same CH<sub>3</sub>CN solutions for Pt-1–Pt-3, and the difference of the TA spectra of Pt-1–Pt-3 from their respective ligands (Supporting Information Figure S8), we tentatively assign the triplet excited states that give rise to the obtained TA to the same triplet excited states that emit, namely, the mixed <sup>3</sup>MLCT/<sup>3</sup>LLCT/<sup>3</sup> $\pi,\pi^*$  states for Pt-1 and <sup>3</sup>MLCT/<sup>3</sup>LLCT states for Pt-2 and Pt-3 in CH<sub>3</sub>CN.

**Reverse Saturable Absorption.** The TA measurements indicate that the triplet excited-state absorption of Pt-1–Pt-3 is stronger than their respective ground-state absorption in the visible to the near-IR spectral region. Therefore, we expect to observe reverse saturable absorption (RSA) in this spectral

region from these complexes. To manifest this, a nonlinear transmission experiment was conducted at 532 nm using 4.1 ns laser pulses in a 2 mm cuvette in  $\text{CH}_2\text{Cl}_2$  solutions for these complexes. The linear transmission of each complex solution was adjusted to 80% at 532 nm in the 2 mm cuvette. The transmission vs incident energy curves for **Pt-1–Pt-3** are presented in Figure 8. With the increased incident energy, the



**Figure 8.** Nonlinear transmission of complexes **Pt-1–Pt-3** and the reference complex **1a**<sup>11</sup> in  $\text{CH}_2\text{Cl}_2$  solution for 4.1 ns laser pulses at 532 nm. The linear transmission is 80%, and the path length of the cuvette is 2 mm.

transmission of these complex solutions decreases dramatically, suggesting the occurrence of RSA. The RSA of these complexes is much stronger than the reference complex (complex **1a** in ref 11) that does not contain the aromatic substituent at the fluorenyl motif.<sup>11</sup> This implies that  $\pi$ -conjugated aromatic electron-withdrawing substituents at the fluorenylacetylde ligands enhance the RSA of the Pt(II) diimine bis(acetylde) complexes.

## CONCLUSIONS

Three platinum(II) bipyridyl complexes with different  $\pi$ -conjugated aromatic electron-withdrawing substituents at the 7-position of the fluorenylacetylde ligands are synthesized, and their photophysical properties and reverse saturable absorption are systematically investigated via spectroscopic techniques. The complexes exhibit ligand-centered  $^1\pi,\pi^*$  transitions below 400 nm, and a broad, structureless  $^1\text{MLCT}/^1\text{LLCT}$  absorption band between 400 and 550 nm in  $\text{CH}_2\text{Cl}_2$  solutions. All complexes emit in fluid solutions at room temperature and at 77 K glassy matrix, with the emitting states being tentatively attributed to  $^3\text{MLCT}/^3\text{LLCT}$  states for **Pt-1–Pt-3** for the phosphorescence in  $\text{CH}_2\text{Cl}_2$ , but to  $^3\pi,\pi^*/^3\text{MLCT}/^3\text{LLCT}$  states for **Pt-1** in  $\text{CH}_3\text{CN}$ . **Pt-1–Pt-3** also exhibit broad triplet excited-state absorption in the visible to the NIR region (425–800 nm for **Pt-1** and **Pt-3**, and 425–725 nm for **Pt-2**) from the same excited states that emit. Because of the stronger triplet excited-state absorption in the visible spectral region, strong RSA occurs at 532 nm for nanosecond laser pulses from all three complexes, which manifests the merit of extending the  $\pi$ -conjugation of the acetylde ligands via aromatic electron-withdrawing substituents.

## ASSOCIATED CONTENT

### Supporting Information

The synthetic details and characterization data for ligands **L-1–L-3** and **(bpy)PtCl<sub>2</sub>**, the concentration-dependent UV–vis absorption spectra of **Pt-1–Pt-3**, the solvent-dependent emission spectra of **Pt-1** and **Pt-3**, the emission spectra of ligands **L-1–L-3**, the concentration- and solvent-dependent emission spectra of **Pt-2** and **Pt-3**, the comparison of the emission spectra of **Pt-2** and **Pt-3** at room temperature and at 77 K, the time-resolved nanosecond transient difference absorption spectra of **Pt-1–Pt-3** and **L-1–L-3**, and the emission parameters of **Pt-1–Pt-3** in different solvents. This material is available free of charge via the Internet at <http://pubs.acs.org>.

## AUTHOR INFORMATION

### Corresponding Author

\*(W.S.) E-mail: [wenfang.sun@ndsu.edu](mailto:wenfang.sun@ndsu.edu). Phone: 701-231-6254. Fax: 701-231-8831.

### Notes

The authors declare no competing financial interest.

## ACKNOWLEDGMENTS

Financial support from the Army Research Laboratory (W911NF-06-2-0032) is acknowledged.

## REFERENCES

- Williams, J. A. G. Photochemistry and Photophysics of Coordination Compounds: Platinum. *Top. Curr. Chem.* **2007**, *281*, 205–268.
- Zhang, J.; Du, P.; Schneider, J.; Jarosz, P.; Eisenberg, R. Photogeneration of Hydrogen from Water Using an Integrated System Based on  $\text{TiO}_2$  and Platinum(II) Diimine Dithiolate Sensitizers. *J. Am. Chem. Soc.* **2007**, *129*, 7726–7727.
- McGarrah, J. E.; Kim, Y.; Hissler, M.; Eisenberg, R. Toward a Molecular Photochemical Device: A Triad for Photoinduced Charge Separation Based on a Platinum Diimine Bis(acetylde) Chromophore. *Inorg. Chem.* **2001**, *40*, 4510–4511.
- Lu, W.; Chan, M. C. W.; Zhu, N.; Che, C.; He, Z.; Wong, K. Structural Basis for Vapoluminescent Organoplatinum Materials Derived from Noncovalent Interactions as Recognition Components. *Chem.—Eur. J.* **2003**, *9*, 6155–6166.
- Chan, S.; Chan, M. C. W.; Wang, Y.; Che, C.; Cheung, K.; Zhu, N. Organic Light-Emitting Materials Based on Bis(arylacetylde)-platinum(II) Complexes Bearing Substituted Bipyridine and Phenanthroline Ligands: Photo- and Electroluminescence from  $^3\text{MLCT}$  Excited States. *Chem.—Eur. J.* **2001**, *7*, 4180–4190.
- Li, Q.; Guo, H.; Ma, L.; Wu, W.; Liu, Y.; Zhao, J. Tuning the Photophysical Properties of  $\text{NN}$  Pt(II) Bisacetylde Complexes with Fluorene Moiety and Its Applications for Triplet–Triplet–Annihilation Based Upconversion. *J. Mater. Chem.* **2012**, *22*, 5319–5329.
- Liu, Y.; Li, Q.; Zhao, J.; Guo, H.  $\text{BF}_2$ -bound Chromophore-Containing  $\text{NN}$  Pt(II) Bisacetylde Complex and Its Application as Sensitizer for Triplet–Triplet Annihilation Based Upconversion. *RSC Adv.* **2012**, *2*, 1061–1067.
- Sun, W.; Zhang, B.; Li, Y.; Pritchett, T. M.; Li, Z.; Haley, J. E. Broadband Nonlinear Absorbing Platinum 2,2'-Bipyridine Complex Bearing 2-(Benzothiazol-20-yl)-9,9-diethyl-7-ethynylfluorene Ligands. *Chem. Mater.* **2010**, *22*, 6384–6392.
- Pritchett, T. M.; Sun, W.; Zhang, B.; Ferry, M. J.; Li, Y.; Haley, J. E.; Mackie, D.; Shensky, W.; Mott, A. G. Excited-State Absorption of a Bipyridyl Platinum(II) Complex with Alkynyl-Benzothiazolylfluorene Units. *Opt. Lett.* **2010**, *35*, 1305–1307.
- Li, Z.; Badaeva, E.; Zhou, D.; Bjorgaard, J.; Glusac, K. D.; Killina, S.; Sun, W. Tuning Photophysics and Nonlinear Absorption of

Bipyridyl Platinum(II) Bisstilbenylacetylide Complexes by Auxiliary Substituents. *J. Phys. Chem. A* **2012**, *116*, 4878–4889.

(11) Liu, R.; Zhou, D.; Azenkeng, A.; Li, Z.; Li, Y.; Glusac, K. D.; Sun, W. Nonlinear Absorbing Platinum(II) Diimine Complexes: Synthesis, Photophysics, and Reverse Saturable Absorption. *Chem.—Eur. J.* **2012**, *18*, 11440–11448.

(12) Liu, R.; Chen, H.; Chang, J.; Li, Y.; Zhu, H.; Sun, W. Pt(II) Diimine Complexes Bearing Carbazolyl-Capped Acetylide Ligands: Synthesis, Tunable Photophysics and Nonlinear Absorption. *Dalton Trans.* **2013**, *42*, 160–171.

(13) Liu, R.; Dandu, N.; Li, Y.; Kilina, S.; Sun, W. Synthesis, Photophysics and Reverse Saturable Absorption of Bipyridyl Platinum(II) Bis(arylfluorenylacetylide) Complexes. *Dalton Trans.* **2013**, *42*, 4398–4409.

(14) Liu, R.; Azenkeng, A.; Zhou, D.; Li, Y.; Glusac, K. D.; Sun, W. Tuning Photophysical Properties and Improving Nonlinear Absorption of Pt(II) Diimine Complexes with Extended  $\pi$ -Conjugation in the Acetylide Ligands. *J. Phys. Chem. A* **2013**, *117*, 1907–1917.

(15) Li, Y.; Liu, R.; Badaeva, E.; Kilina, S.; Sun, W. Long-Lived  $\pi$ -Shape Platinum(II) Diimine Complexes Bearing 7-Benzothiazolylfluorene-2-yl Motif on the Bipyridine and Acetylide Ligands: Admixing  $\pi, \pi^*$  and Charge-Transfer Configurations. *J. Phys. Chem. C* **2013**, *117*, 5908–5918.

(16) Liu, R.; Azenkeng, A.; Li, Y.; Sun, W. Long-Lived Platinum(II) Diimine Complexes with Broadband Excited-State Absorption: Efficient Nonlinear Absorbing Materials. *Dalton Trans.* **2012**, *41*, 12353–12357.

(17) Castellano, F. N.; Pomestchenko, I. E.; Shikhova, E.; Hua, F.; Muro, M. L.; Rajapakse, N. Photophysics in Bipyridyl and Terpyridyl Platinum(II) Acetylides. *Coord. Chem. Rev.* **2006**, *250*, 1819–1828.

(18) Hissler, M.; Connick, W. B.; Geiger, D. K.; McGarrah, J. E.; Lipa, D.; Lachicotte, R. J.; Eisenberg, R. Platinum Diimine Bis(acetylide) Complexes: Synthesis, Characterization, and Luminescence Properties. *Inorg. Chem.* **2000**, *39*, 447–457.

(19) Whittle, C. E.; Weinstein, J. A.; George, M. W.; Schanze, K. S. Photophysics of Diimine Platinum(II) Bis-Acetylide Complexes. *Inorg. Chem.* **2001**, *40*, 4053–4062.

(20) Wadas, T. J.; Lachicotte, R. J.; Eisenberg, R. Synthesis and Characterization of Platinum Diimine Bis(acetylide) Complexes Containing Easily Derivatizable Aryl Acetylide Ligands. *Inorg. Chem.* **2003**, *42*, 3772–3778.

(21) Pomestchenko, I. E.; Castellano, F. N. Solvent Switching between Charge Transfer and Intraligand Excited States in a Multichromophoric Platinum(II) Complex. *J. Phys. Chem. A* **2004**, *108*, 3485–3492.

(22) Pomestchenko, I. E.; Luman, C. R.; Hissler, M.; Ziesel, R.; Castellano, F. N. Room Temperature Phosphorescence from a Platinum(II) Diimine Bis(pyrenylacetylide) Complex. *Inorg. Chem.* **2003**, *42*, 1394–1396.

(23) Guo, H.; Ji, S.; Wu, W. H.; Wu, W. T.; Shao, J.; Zhao, J. Long-Lived Emissive Intra-Ligand Triplet Excited States ( $^3IL$ ): Next Generation Luminescent Oxygen Sensing Scheme and a Case Study with Red Phosphorescent Diimine Pt(II) Bis(acetylide) Complexes Containing Ethynylated Naphthalimide or Pyrene Subunits. *Analyst* **2010**, *135*, 2832–2340.

(24) Guo, H.; Muro-Small, M. L.; Ji, S.; Zhao, J.; Castellano, F. N. Naphthalimide Phosphorescence Finally Exposed in a Platinum(II) Diimine Complex. *Inorg. Chem.* **2010**, *49*, 6802–6804.

(25) Sun, H.; Guo, H.; Wu, W.; Liu, X.; Zhao, J. Coumarin Phosphorescence Observed with  $\hat{N}N$  Pt(II) Bisacetylide Complex and Its Applications for Luminescent Oxygen Sensing and Triplet–Triplet–Annihilation Based Upconversion. *Dalton Trans.* **2011**, *40*, 7834–7841.

(26) Liu, Y.; Wu, W.; Zhao, J.; Zhang, X.; Guo, H. Accessing the Long-Lived Near-IR-emissive Triplet Excited State in Naphthalenediimine with Light-Harvesting Diimine Platinum(II) Bisacetylide Complex and Its Application for Upconversion. *Dalton Trans.* **2011**, *40*, 9085–9089.

(27) Hudson, Z. M.; Sun, C.; Harris, K. J.; Lucier, B. E. G.; Schurko, R. W.; Wang, S. Probing the Structural Origins of Vapochromism of a Triarylboron-Functionalized Platinum(II) Acetylide by Optical and Multinuclear Solid-State NMR Spectroscopy. *Inorg. Chem.* **2011**, *50*, 3447–3457.

(28) Kannan, R.; He, G. S.; Lin, T.; Prasad, P. N.; Vaia, R. A.; Tan, L. Toward Highly Active Two-Photon Absorbing Liquids. Synthesis and Characterization of 1,3,5-Triazine-Based Octupolar Molecules. *Chem. Mater.* **2004**, *16*, 185–194.

(29) Raymond, J. E.; Bhaskar, A.; Goodson, T., III; Makiuchi, N.; Ogawa, K.; Kobuke, Y. Synthesis and Two-Photon Absorption Enhancement of Porphyrin Macrocycles. *J. Am. Chem. Soc.* **2008**, *130*, 17212–17213.

(30) Kannan, R.; He, G. S.; Yuan, L.; Xu, F.; Prasad, P. N.; Dombroskie, A. G.; Reinhardt, B. A.; Baur, J. W.; Vaia, R. A.; Tan, L. Diphenylaminofluorene-Based Two-Photon-Absorbing Chromophores with Various  $\pi$ -Electron Acceptors. *Chem. Mater.* **2001**, *13*, 1896–1904.

(31) Thomas, K. R. J.; Velusamy, M.; Lin, J. T.; Chuen, C.; Tao, Y. Chromophore-Labeled Quinoxaline Derivatives as Efficient Electroluminescent Materials. *Chem. Mater.* **2005**, *17*, 1860–1866.

(32) Demas, J. N.; Crosby, G. A. Measurement of Photoluminescence Quantum Yields. Review. *J. Phys. Chem.* **1971**, *75*, 991–1024.

(33) Van Houten, J.; Watts, R. J. Temperature Dependence of the Photophysical and Photochemical Properties of the Tris(2,2'-bipyridyl)ruthenium(II) Ion in Aqueous Solution. *J. Am. Chem. Soc.* **1976**, *98*, 4853–4858.

(34) Sun, W.; Zhu, H.; Barron, P. M. Binuclear Cyclometalated Platinum(II) 4,6-Diphenyl-2,2'-bipyridine Complexes: Interesting Photoluminescent and Optical Limiting Materials. *Chem. Mater.* **2006**, *18*, 2602–2610.

(35) Kubista, M.; Sjöback, R.; Eriksson, S.; Albinsson, B. Experimental Correction for the Inner-Filter Effect in Fluorescence Spectra. *Analyst* **1994**, *119*, 417–419.